LIGHTNING LOCATION SYSTEMS (LLS)

Gerhard Diendorfer

OVE-ALDIS

g.diendorfer@ove.at

Kahlenberger Str. 2A, 1190 Vienna, Austria

Abstract – Nowadays various techniques are employed to locate lightning activity over large areas. Electric and/or magnetic field sensors in the VLF, LF and VHF frequency ranges measure the lightning radiated electromagnetic fields. For locating ground strike points magnetic direction finding (MDF), time-of-arrival (TOA), or a combination of both (MDF+TOA) is employed. Major difference between those techniques is the minimum number of sensor required to calculate a stroke location. Network configuration (mean baseline between sensors, network geometry) and the type of sensors employed strongly affect the achievable detection efficiency (DE) and the resulting peak current distribution. Normally it is the strokes with small peak currents that are missed by lower DE networks and this results in a bias of the peak current distribution to higher values. In this paper we present some results of model calculations and performance evaluation of a LLS based on directly measured lightning to an instrumented tower in Austria.

1   INTRODUCTION

The following document is partially based on a final draft version of a CIGRE brochure entitled "*Cloud-to-Ground Lightning Parameters Derived from Lightning Location Systems*" prepared by CIGRE TF C4.404 "Lightning Location System Data for Engineering Applications". As the convener of this Task Force (TF C4.404) I have to acknowledge major contributions to this document by Ken Cummins (Vaisala), Vladimir A. Rakov (Univ. of Florida) and Wolfgang Schulz (ALDIS).

Since information about cloud to ground lightning (CG) is of primary interest for lightning protection applications this document is limited to the discussion of lightning detection systems that operate on surface-propagated VLF/LF signals produced by CG discharges. The sensors in these systems are typically separated by 50-400 km, employing measurements of the lightning radiated magnetic and/or electric field. Ground strike points of CG discharges are located by using various forms of magnetic direction finding (MDF), time-of-arrival (TOA), and combinations thereof. More comprehensive discussions including other detection methods and frequency ranges can be found in Cummins and Murphy (2000) and Rakov and Uman (2003).

Some key lightning parameters which are of main importance for power engineering and lightning protection are inferable from LLS data. Some of these data are affected by the configuration setting of the LLS and the actual performance of the LLS. This includes classification of lightning type (CG vs. cloud discharges) and combining CG strokes into flashes.

1.1   Magnetic Direction-Finders (MDFs)

For CG discharges the initial field peak of the radiated magnetic (and electric) field occurs at a time, when the upward propagating return stroke has reached a height of a few hundred meters. MDF systems determine the direction just at the time of initial peak field incidence from signals measured by crossed loop antennas. Hence the resulting direction vector points as closely as possible to the location where the CG stroke attached to ground. Sampling of the electric field is also required at this time to determine the stroke polarity (Krider et al., 1976, 1980).

In a typical network three or more sensors report a discharge and an optimization which minimizes the "angle disagreement" between the reporting sensors can be employed as shown in Fig. 1.
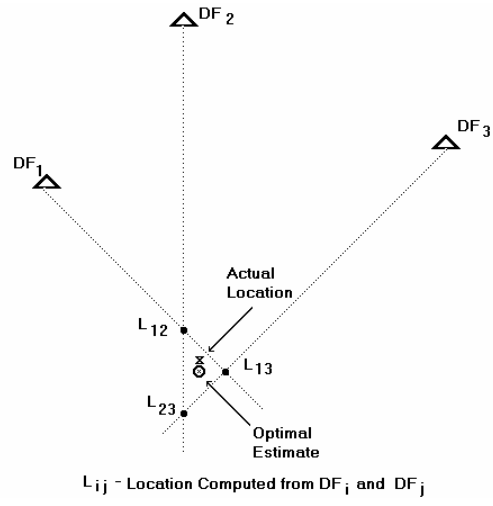
Fig. 1: Optimal location algorithm for direction finding (adopted from Cummins and Murphy, 2000)

Proper location of lightning with MDF sensors requires implementation of the so called "site error correction" in the location algorithm. Local sensor site conditions (nearby objects, metal fences, buried cables or other conducting installations) are causing a more or less significant change in the direction of field incidence, which can be up to 10° or even more for a poor sensor site. It is possible to determine these systematic site errors for each MDF sensor site from historical data in form of a correction function $\Delta\varphi = f(\varphi)$ and consider these correction in the location algorithm.

An example of such a typically two-sinusoidal site error function is shown in Fig. 2.
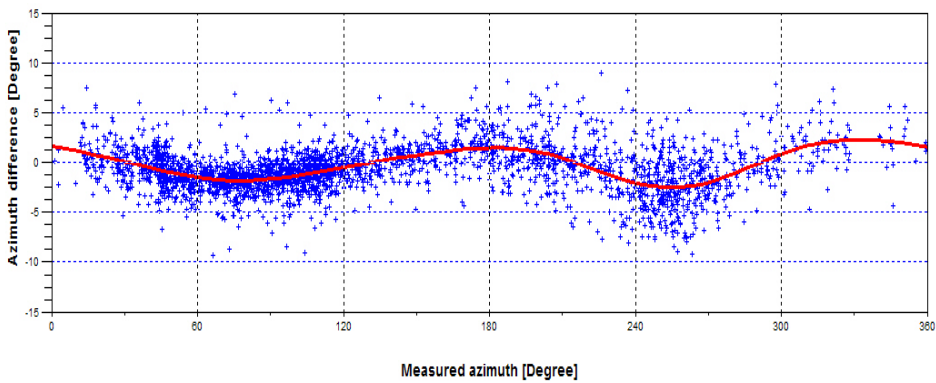
Fig. 2: Typical site error function of a MDF sensor. (+) Error values determined from historical data, solid line represents n-harmonic fit to the point data and is used as error correction function in the location algorithm

1.2 Time-of-Arrival (TOA) Systems

Lightning radiated field propagates in all directions with the speed of light (3.10^8 m/s) and hence we observe differences in the arrival time at sensors located at various distances from the striking point. A constant difference in the arrival time at two stations defines a hyperbola, and multiple stations provide multiple hyperbolas whose intersections define the source location (see Fig. 3). Locating lightning by TOA method requires precise synchronization of the sensors, which is available from GPS satellite signals today, and a minimum of three sensors reporting a stroke. Under some geometrical conditions, curves produced from only three sensors will result in two intersections, leading to an ambiguous location as shown in Fig. 4. This problem is generally avoided if four sensors are required to locate a discharge.
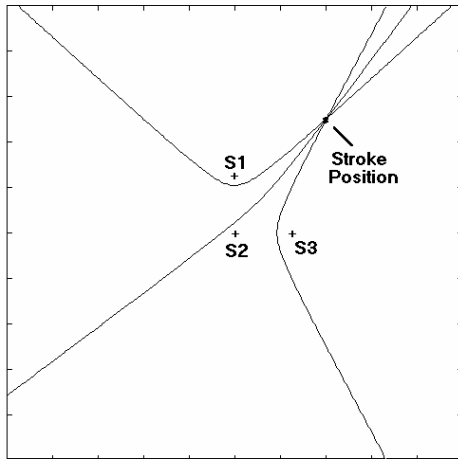
Fig. 3: Hyperbolic intersection method for locating lightning using three sensors. (Cummins and Murphy, 2000)
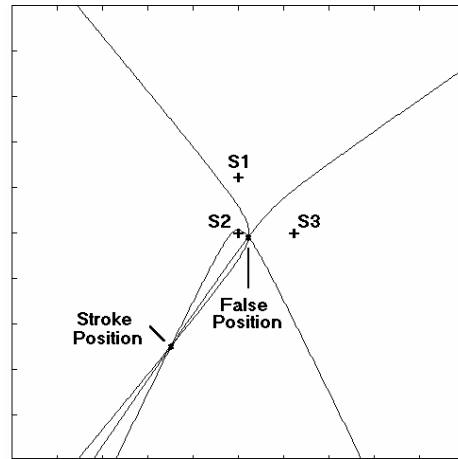
Fig. 4: Example of an ambiguous location for a three-sensor hyperbolic intersection. (Cummins and Murphy, 2000)

1.3   Combined Direction Finding and Time-of-Arrival (MDF+TOA)

A method combining direction-finding and time-of-arrival and referred to as IMPACT (IMProved Accuracy using Combined Technology) method was introduced by Global Atmospherics in the early 1990's. In this approach, direction finding provides azimuth information and absolute arrival time provides range information. The combined MDF+TOA method has redundant information which allows an optimized estimate of the three unknown parameters -- latitude, longitude, and discharge time, even when only two sensors provide both timing and angle information. The MDF+TOA location algorithm can utilize information from any combination of direction finding, TOA, or combined (MDF+TOA) sensors.

1.4   Classification of Lightning Type

All LLS sensors are exposed to electric and magnetic field signals from various discharge types during thunderstorm activity. Although the fields produced by return strokes in CG flashes are by far the largest VLF/LF lightning "signal", other components of in-cloud and intra-cloud flashes are also detected in this frequency range, especially from sensors nearby the storm. It is a complex task to correctly identify and classify each lightning emitted electromagnetic pulse. Classification is either done at the sensor level by including a set of "waveform criteria" that reject events that differ in those features from usual strokes of CG flashes (Krider et al, 1980) or by the central processor (CP), when waveform parameters are sent by the sensor to the CP and classification is based on a combined analyses of those parameters from a set of sensors used for locating the stroke. Sensors are frequently reporting different waveform parameters as a result of signal attenuation when propagating over ground of finite conductivity. Discharges are currently classified using a Peak-to-zero (PTZ) duration criterion, which is the time from the initial peak in the waveform until the first zero-crossing after this peak. Discharges with small PTZ values are classified as cloud discharges. The specific PTZ values (separate for positive and negative discharges) as well as criteria for the classification procedure when PTZ values of sensors are inconsistent for a given discharge (some sensors indicate a CG and others indicate a CC discharge) are configurable parameters at the central processor (e.g. LP2000), and has an effect on the amount of misclassification.

Depending on the network setting and network layout there is some probability of misclassified events, primarily in terms of cloud discharges being called small positive CG strokes. Recent studies in the US employing GPS-synchronized video cameras (Biagi et al., 2007) using NLDN data from 2003-2004 have shown that most positive discharges with peak current below 10 kA in the southern U.S. are cloud discharges, whereas nearly all positive discharges above 20 kA are CG. Misclassification rate for negative discharges was very small in this study. The quality of stroke classification has more or less pronounced direct implications for lightning parameters of positive flashes derived from LLS.

1.5 Grouping CG Strokes into Flashes

The LLS locates the individual strokes in a multi-stroke flash completely independent from each other and various methods can be used to group strokes into flashes and this will affect several derived lightning parameters. Older systems manufactured by LLP and based on the "APA" central processor (prior to 1995) employed an angle-based algorithm where each DF sensor counted all strokes that occurred within ±2.5 degrees of the first stroke for a period of one second after the first stroke. The assigned flash multiplicity was simply the largest number of strokes detected by any DF in such a network.

Other grouping algorithms group strokes into flashes using a spatial and temporal clustering algorithm illustrated in Fig. 5. Strokes are added to any active flash for a specified time period (usually 1 second) after a first stroke, as long as the additional strokes are within a specified clustering radius (usually 10 km) of the first stroke and the time interval from the previous stroke is less than a maximum interstroke interval (usually 500 ms). Additionally, in modern central processors developed by Global Atmospherics (LP2000) and Vaisala (CP8000), if a stroke is located more than the clustering radius from the first stroke but is not clearly separated from that stroke because their location confidence regions overlap, then the stroke is included in the flash. Depending on the system configuration, strokes may be counted in the multiplicity even if they have a polarity that is opposite that of the first stroke. Finally, the systems generally allow the user to determine if the assigned flash peak current is the value associated with the first return stroke or the largest stroke in the flash.
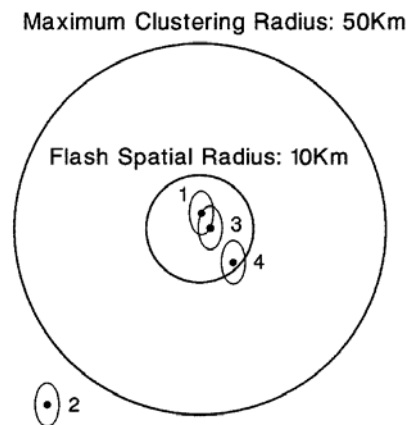
Fig. 5: Spatial clustering method for grouping strokes into flashes (Cummins et al., 1998)

Clearly, the grouping algorithm can have an affect on the measured flash multiplicity and peak current distribution. In a 10-year analysis of lightning data in Austria (Schulz et al., 2005), a 20% decrease in estimated negative flash multiplicity was observed when changing from the angle-based flash algorithm to the spatial clustering algorithm, using the default parameters.

Also, the flash peak current distribution will clearly change depending on the choice of "first stroke" or "largest stroke" as the flash peak current. When the largest stroke amplitude was assigned as the flash amplitude Schulz et al. (2005) observed a +14% increase in the median peak current for negative flashes and +4% increase for positive flashes.

There is an interesting and important implication for lightning protection analysis associated with the meteorologically-based flash grouping algorithms discussed above. Lightning "flash" reports typically relate to the location of the first return stroke and a count of all strokes (multiplicity) associated with this meteorological event. Today "Flash counts" or GFD (ground flash density) are used as a quantitative replacement for the thunderday or thunderhour estimates of lightning exposure of an object. However, in order to assess fully the lightning threat to a specific asset or structure, one must understand the nature of multiple ground contacts that are frequently associated with a single flash. On average, there appears to be about 1.5-1.7 strike points for each CG flash. Hence, for a complete evaluation of the threat from CG lightning, one should use the area density of ground strike points as GFD. At the moment, commercial LLS's

are limited in that they can resolve only strike points that are separated by several hundred meters, but this is already much less than the 10 km radius used for clustering the strokes of the meteorological flash event.

1.6   Peak current estimate

According to the transmission line model (TL) introduced by Uman et al. (1975), the peak current I_p is related to the peak field E_p by following expression:

$$I_p = \frac{2.\pi.\varepsilon_0.c^2.D}{v}.E_p \qquad (1)$$

where D is the horizontal distance between the lightning channel and the observation point, v is the return stroke speed, and c is the speed of light and assuming that v=const, the ground is perfectly conducting, and the return-stroke front has not reached the top of the channel.

For a typical return stroke velocity of 1.10^8 m/s and a reference distance D = 100 km, Eq.(1) becomes

$$I_p \text{ [kA]} = 5. E_p \text{ [V/m]}. \qquad (2)$$

This linear relation is used to infer lightning peak currents from measured peak fields. Often the peak current is inferred from the so called LLP-Units, which are directly proportional to the peak electric field in V/m. Given by the manufacturer Vaisala the following relation exists between the LLP-Units (sensor output signal) and the electric field at the sensor site.

$$52 \text{ V/m} \triangleq 1158 \text{ LLP-Units} \qquad (3)$$

Combining Eq.(2) and Eq.(3) results in the often used direct conversion of the range normalized signal strength $\overline{RNSS}$ in so-called "LLP-Units" to peak current in kA in the form of

$$I_p\text{[kA]} = SNF * \overline{RNSS} \quad \text{[LLP– Units]} \qquad (4)$$

where SNF is the Signal Normalization Factor (e.g. SNF=0,23) and $\overline{RNSS}$ is the mean value of all $RNSS_i$ (sensor signal strengths range normalized to a distance of 100 km of the i-th sensor participating in the location).

The range normalized signal strength ($RNSS_i$) of the i-th sensors is calculated using Eq. 5 (see Cummins et al. 1998). In this equation SS_i is the raw signal strength and D_i is the distance in km from the i-th sensor to the estimated ground strike point. Parameters b and L are taking into account effects of field propagation over ground of finite conductivity.

$$RNSS_i = SS_i * \left(\frac{D_i}{100}\right)^b * \exp\left(\frac{D_i - 100}{L}\right) \qquad (5)$$

When we assume a purely inverse-distance dependency of the lightning radiated field, which is valid only in case of infinite ground conductivity, we have to set b = 1.0 and the space constant L to a very large value (e.g. $L = 10^5$ km). Different values for the attenuation constants b have been proposed in literature, e.g. b= 1.13 by Orville (1991) or b= 1.09 by Idone et al. (1993). Herodotou et al. (1993) and Cramer et al. (2004) have shown the importance of applying an appropriate attenuation model and that a model applying a space constant L fits reality better than an exponential attenuation model. In the EUCLID network parameters SNF, b and L were set to SNF=0.23, b=1.0 and $L=10^5$ until March 2005 which means no consideration of any attenuation effects. EUCLID is a joint network of several national networks in Europe, including the Austrian network ALDIS (see www.euclid.org). Based on a comprehensive data analysis those parameters were changed to SNF=0.183; b=1.0 and L=1000 in March 2005.

Due to the high variability of some key parameters such as the return stroke speed (see Rakov, 2007) and propagation effects, it is not possible to determine the lightning current accurately from the remotely measured electric or magnetic

field for any given event. Nevertheless it has been shown by Rachidi et al., 2004, that the statistical estimation (e.g. in terms of mean values and standard deviations) is possible.

It is worth to note that the linear relationship used to infer the peak current from the peak field is not solely based on the TL model. Existence of such a linear relationship of those two parameters has been validated by simultaneous measurements of currents and fields from triggered lightning and lightning to towers (Jerauld et al. 2005, Diendorfer et al. 2002).

2   NETWORK DETECTION EFFICIENCY (DE)

DE is defined as the percentage of discharges (of a given type) that are reported by the LLS. Some specific examples are stroke DE_s (the fraction of all strokes, including first and subsequent) and subsequent stroke DE_{su} (excludes first strokes). As a flash is reported (detected) if at least one stroke (first or subsequent) is detected the flash DE_f can be much higher than any form of stroke DE.

A schematic sensor DE function DE_i – not to be mixed up with the DE of a multi-sensor network - is illustrated in Fig. 6 and defines the probability of a sensor S_i to detect a given field signal strength SS_i reaching the remote sensor site. Note that there is a minimum signal strength (detection threshold) below which no events are detected, and that the maximum detectability is not reached until the signal is a bit larger than the detection threshold. Note also that as signal strength increases further, the DE_i decreases and eventually returns to zero when the sensor "over-ranges" and is no longer able to provide reliable information. Since each sensor that detects a specific stroke will be at a different distance, they may all have different sensor DE_i values for this stroke. Using the assumption that each sensor responds independently from all other sensors these DE_i values are independent for each sensor S_i.
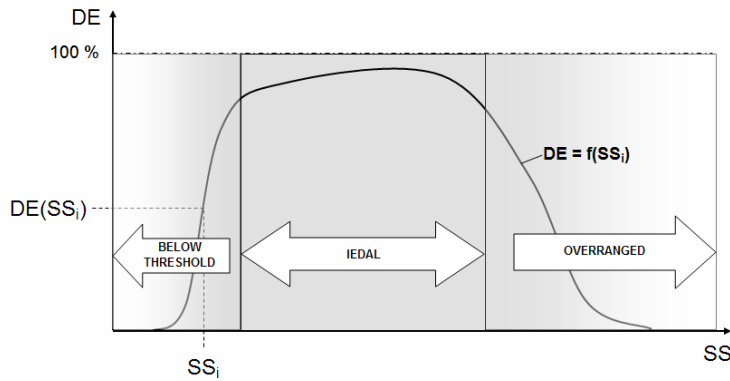
Fig. 6: Sensor DE as a function of signal strength SS (schematic)

Based on this assumption, and by defining the probability of sensor S_i NOT detecting the event as $Q_i = 1-DE_i$, then the probability of a specific combination of sensors detecting the event is simply the product of the appropriate DE_i and Q_i values for all available sensors. For example, the probability that a stroke with current I_0 is detected by a minimum of 2 sensors of a 3 sensor network, is

Prob(detection of a stroke with peak current I_0 in a three sensor network) =

$$
\begin{array}{ll}
[DE_1(I_0,r_1)*DE_2(I_0,r_2)*Q_3(I_0,r_3)] + & \text{.... detected by \#1 AND \#2, NOT by \#3} \\
[DE_1(I_0,r_1)*Q_2(I_0,r_2)*DE_3(I_0,r_3)] + & \text{.... detected by \#1 AND \#3, NOT by \#2} \quad (6) \\
[Q_1(I_0,r_1)*DE_2(I_0,r_2)*DE_3(I_0,r_3)] + & \text{.... detected by \#2 AND \#3, NOT by \#1} \\
[DE_1(I_0,r_1)*DE_2(I_0,r_2)*DE_3(I_0,r_3)] & \text{.... detected by \#1 AND \#2 AND \#3}
\end{array}
$$

as the signal strength at the sensor site is a function of I_0 and the distance r_i.

Using this construct, it is possible to determine the probability of detection for any specific number of sensors in a network of arbitrary size and create a model to calculate the DE of a detection network over a given region, when an appropriate peak current distribution and sensor DE functions are assumed.

Based on such a model we have calculated the DE for a six-sensor network to demonstrate the effect of sensor baseline, applied location method and temporarily outage of one sensor. The sensors are assumed to be located at the corners and the center of a pentagon as shown in Fig. 5. To demonstrate the effect of baseline length we have set the radius of the pentagon to 150, 200 and 300 km, respectively. To analyze the effect of a sensor outage we have removed the central sensor (#6) or one of the corner sensors (#5). For each network configuration we have calculated the overall DE for the different location methods, requiring 2, 3 or 4 sensors. The assumed sensor sensitivity is what would typically be used for sensor baselines of 150-200 km and kept unchanged for all model calculations. Some examples of the 15 different network settings considered are shown in Fig. 8. Plots of the model calculated DE of a combined MDF/TOA network and a pure TOA network requiring 4 sensors for a location are presented. Table 1 summarizes the overall DE results within a region of 600 km x 600 km (150 and 200 km baseline networks) and 800 km x 800 km (300 km baseline network) area for all the 15 combinations.
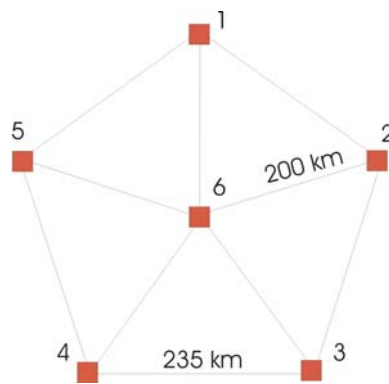
Fig. 7: Outline of Test Network (sensors are located at centre and corners of a pentagon) with baseline of 200 km being changed to150 km and 300 km, respectively, in the model simulations

Table 1: Results of model calculated DE of various network settings

Network/Sensor status	Number of sensors required to get a location		
	2	3	4
Sensor Baseline 200 km All 6 sensors in operation	96,5 % (Fig. 8a)	90,4 %	76,6 % (Fig. 8b)
Sensor Baseline 200 km Centre sensor removed	94,0 %	81,2 %	58,3 %
Sensor Baseline 200 km One corner sensor removed	94,5 % (Fig. 8c)	84,0 %	60,3 % (Fig. 8d)
Sensor Baseline 150 km All 6 sensors in operation	97,0 %	92,2 %	80,6 %
Sensor Baseline 300 km All 6 sensors in operation	89,5 %	76,5 %	56,3 %

It is interesting to note, that for a given baseline of 200 km the overall DE values are in a range between 58,3 % and 96,5 %, depending on applied location method and proper operation of all available sensors
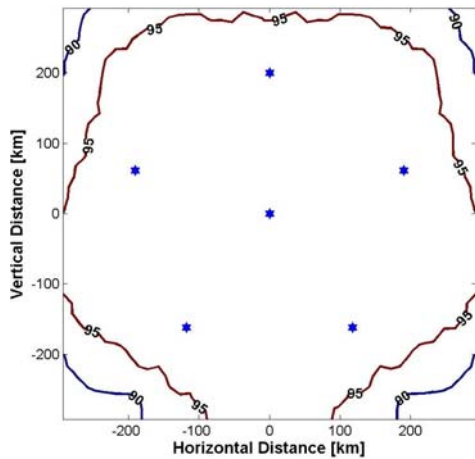
Fig. 8.a: Simulation for a 6 sensor network, Baseline 200 km, MDF+TOA method with 2 sensors required DE = 96,5 % (600 km x 600 km area)
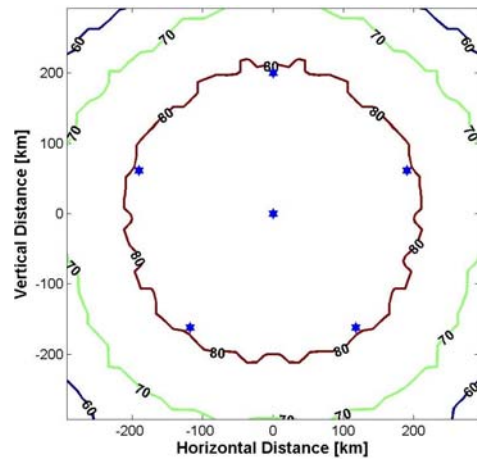
Fig. 8.b: Simulation for a 6 sensor network, Baseline 200 km, TOA method with 4 sensors required DE = 76,6 % (600 km x 600 km area)
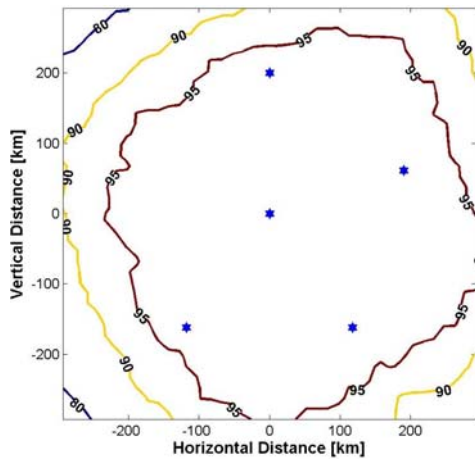
Fig. 8.c: Simulation for a 5 sensor network (corner sensor #5 removed), Baseline 200 km, MDF+TOA method with 2 sensors required DE = 94,5 % (600 km x 600 km area)
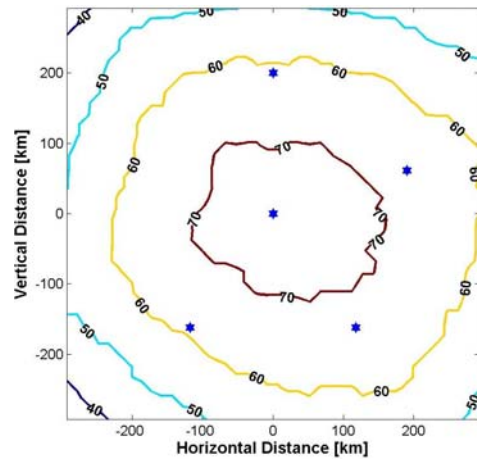
Fig. 8.d: Simulation for a 5 sensor network (corner sensor #5 removed), Baseline 200 km, TOA method with 4 sensors required DE = 60,3 % (600 km x 600 km area)

Validity of this model calculations has been proven by reprocessing a given set of sensor raw data of one summer month of the Austrian lightning location system ALDIS with similar system configurations. By enabling and disabling to usage of the angles reported by the sensors and specifying the number of sensors required for a location in the LP2000 configuration we have simulated different network types. Relatively to a combined MDF/TOA network with 2 sensors required about 30 % of the flashes were missed by the same network when configured as TOA network with 4 sensors required. Median of neg. peak currents increased from -9.7 kA to -12 kA as a result of the missed small events.

3   LLS PERFORMANCE ANALYSIS BASED ON LIGHTNING TO AN INSTRUMENTED TOWER

An appropriate set of ground truth reference data is fundamental for any performance evaluation of LLS. Ideally such a data set includes precise knowledge of time, type of discharge (CG versus CC), location (latitude/longitude) and peak current of all the strokes in all CG flashes within a given area and time period. Unfortunately today no such complete data set is practically available. Analyzing lightning to an elevated tower is a good approach, although the majority of the discharges to elevated objects is initiated by upward propagating leaders similar to triggered lightning and thus different from typical discharges to ground, which are initiated by a downward propagating stepped leaders.

Lightning to elevated objects typically starts with an upward leader establishing an initial continuous current (ICC) with a duration of some hundreds of milliseconds and an amplitude of some tens to some thousands of amperes. Often current pulses are superimposed on the slowly varying continuous current and these pulses are called α-pulses (Fig. 9). After the cessations of the ICC, one or more downward leader/upward return stroke sequences, similar to subsequent strokes in CG lightning, may occur – the associated current pulses are called β-pulses (Fig. 9 and Fig. 10).
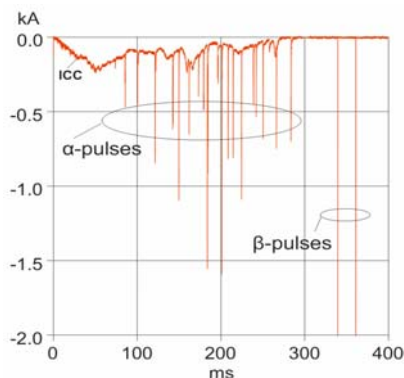
Fig. 9:   Overall current record of upward lightning from an elevated tower
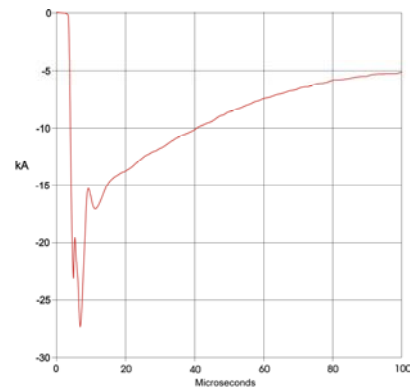
Fig. 10:   β-pulse current waveform (most similar to subsequent strokes in CG lightning and hence used for LLS performance analysis)

As these β-pulses are a good representation of subsequent strokes in CG lightning, we are only using this subset of tower recorded lightning data for the performance analysis of the LLS.

During the period 2000 – 2005 a total of 110 flashes with at least one β-pulse following the ICC sequence were measured at the Gaisberg tower in Austria. Peak current distribution of these tower measured β-pulses is shown in Fig. 11 with a median of 9.6 kA (N=476, σ_{log}=0.23). The smallest β-pulse peak current measured was 2.1 kA and the maximum was 68 kA (Note: the 68 kA pulse was above the 40 kA measuring limit of Gaisberg instrumentation and 68 kA is the peak current inferred by the LLS for that event).
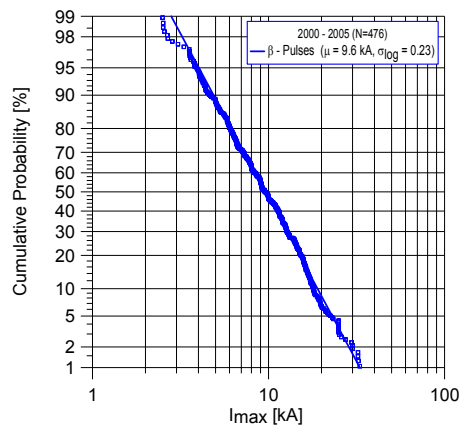
Fig. 11: Distribution of β-pulse peak currents measured at the top of Gaisberg tower 2000 - 2005

3.1 Flash DE$_f$

108 out of the 110 flashes with at least one β-pulse were detected by the EUCLID lightning detection network confirming a flash DE of 98%. This is actually a lower bound of DE$_f$ as we have been unable to correlate the 2 missed flashes because of a GPS failure at the Gaisberg site and there is some chance that those two flashes have been located by the EUCLID network too.

3.2 Subsequent Stroke DE$_{su}$

As in upward lightning from a tower there is nothing similar to a first stroke in downward neg. lightning to ground, stroke detection analysis is limited to the DE$_{su}$ of subsequent strokes (β-pulses). In agreement with the model concept of detecting a stroke, described in section 2, the Stroke DE$_{su}$ is smaller then flash DE$_f$ for small peak current discharges and increases for strokes of larger peak currents as shown in Fig. 12.
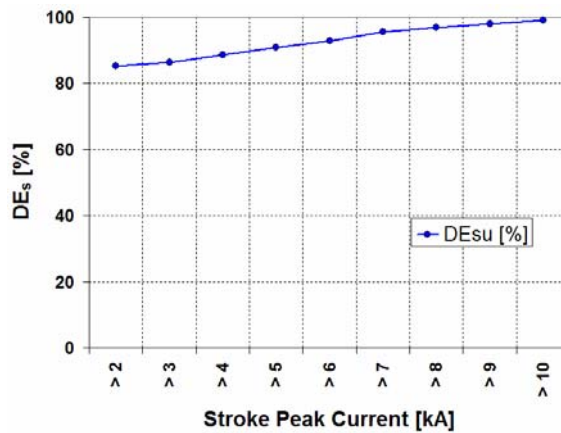
Fig. 12: Subsequent stroke DE$_{su}$ as a function of measured peak current at the Gaisberg tower (N=476)

From all (N=476) directly measured β-pulses the LLS detected 406 and therefore missed 70 strokes equal to a DE$_{su}$ of 85,3%. Achievable DE$_1$ of the same network for first strokes should be at least as good as DE$_{su}$ or even higher assuming that peak currents of first strokes in downward CG lightning are higher than the peak currents of subsequent strokes. The observed excellent performance of the LLS is primarily a result of 5 sensors (4 of them being IMPACT sensors providing angle and time) within a short range of less then 150 km (see Table 2) .

Table 2: Type and distance of the five EUCLID sensors next to the Gaisberg tower

Sensor Location	Sensor Type	Sensor distance to Gaisberg Tower [km]
Eggelsberg (A)	IMPACT 141T	31
Niederoeblarn (A)	IMPACT 141T	77
Schwaz/T (A)	IMPACT ES	116
Muenchen (D)	LPATS III	118
Noetsch (A)	IMPACT 141T	142

A similar analysis by Jerauld et al. (2005) of the U.S. NLDN with 2001 - 2003 triggered lighting data in Florida resulted in a DE$_{su}$ of 60 % and a DE$_f$ of 84 %. These somewhat lower values are a result of significantly longer distances to the next nearest sensor around the triggering site. Only one sensor is within a range of 200 km making it difficult to locate small amplitude strokes.

3.3 Location Accuracy

A median location error of 368 m and a standard deviation of 768 m were determined for the 406 located β-pulses, as shown in Figure 13.
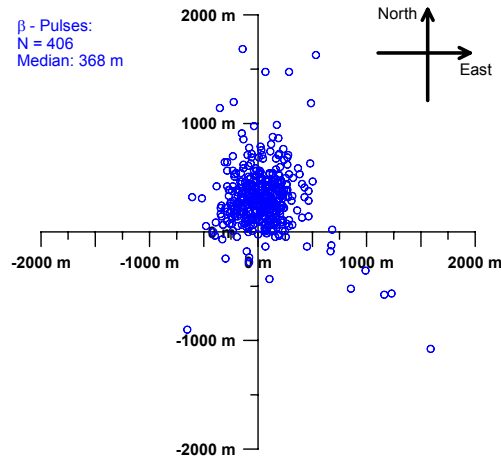
Fig. 13: Plot of EUCLID stroke locations for 406 β-pulses during 2000–2005 (Origin corresponds to the tower location)

The plot in Fig. 13 exhibits a bias of the EUCLID stroke locations by about 300 meters to the north. Reasons for that bias (systematic error) are assumed to be a combination of (1) timing errors as a result of pulse propagation over ground of finite conductivity and different sensor bandwidth and (2) a result of propagation elongation caused by field propagation over high mountains (Schulz and Diendorfer, 2000).

Location errors exceeding 2 km for single events were observed for strokes located by only two or three sensors or when the location was calculated by the LP based on erroneously grouped sensor messages resulting from discharges that occurred almost simultaneously at two separate locations.

For triggered lightning in Florida Jerauld et al. (2005) found a median location error of 600 m.

3.4 Peak Current Estimate

A strong positive linear correlation between the tower measured peak currents I_{GB} and the EUCLID estimated peak currents I_{EUCLID} is observed in Fig. 14, although for some individual events significant differences between directly measured peak current at the tower top and the LLS inferred peak current is obvious. Peak radiated field of a stroke depends on the return stroke speed v (see Eq.(1)) which is observed to have a high variability (Rakov, 2007).

Overall the ground truth measurements at the Gaisberg tower are in good agreement with results of model estimates of DE and LA of the EUCLID network in the area of the tower site. Some first results of recent correlated measurements of currents at the tower and electromagnetic fields at close and far distance (80km) will be presented at this conference in a separate paper by Pichler et al. (2007).
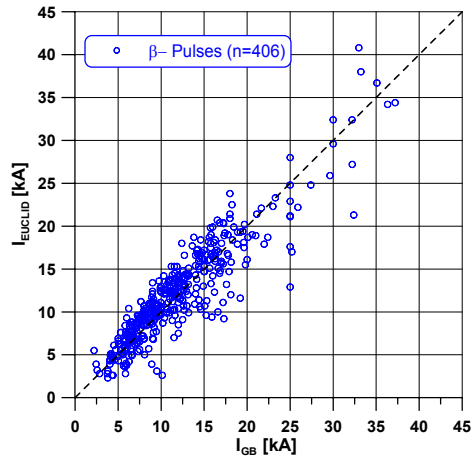
Fig. 14:   EUCLID peak currents plotted versus peak currents measured at the Gaisberg tower during the season 2000–2005.

4   CONCLUSION

Locating lightning is a complex task and involves numerous distinct areas as lightning physics, propagation of transient electromagnetic fields over finitely conducting ground, applied sensor technology, local site conditions of each sensor, applied location method, parameterization of location algorithm and finally the reliability of communication between sensor and central analyzer. Anyone of these mentioned areas might affect more or less the resulting lightning data gathered by a LLS. To avoid misinterpretations of LLS lightning data a close cooperation of the system manufacturer , the system operator and the data user is highly recommended.

As shown in this presentation we can today achieve a flash DE of close to 100% with a proper designed and operated network, nevertheless several questions remain open and require further experimental research and confirmation. Quality of discharge type classification (GC versus CC) is a critical factor when CG/CC ratios are used for example as a parameter to identify severe storms. Today peak currents of positive lightning are inferred by using the same E/I relationship (Eq.(4)) as for negative discharges. Sufficient experimental data from triggered lightning and natural lightning to towers is only available for negative lightning with relatively small amplitudes (< 30 kA or so).

5   REFERENCES

[1]   Biagi, C. J., K. L. Cummins, K. E. Kehoe, and E. P. Krider (2007), National Lightning Detection Network (NLDN) performance in southern Arizona, Texas, and Oklahoma in 2003–2004, J. Geophys. Res., 112, D05208, doi:10.1029/2006JD007341.

[2]   Cramer, J. A., K. L. Cummins, A. Morris, R. Smith, and T. R. Turner (2004), Recent upgrades to the U.S. national lightning detection network, 18th ILDC, Helsinki

[3]   Cummins, K. L., and M. J. Murphy (2000), Overview of Lightning Detection in the VLF, LF, and VHF Frequency Ranges, 2000 ILDC, Tucson, Arizona

[4]   Diendorfer, G., W. Hadrian, F. Hofbauer, M. Mair, and W. Schulz (2002), Evaluation of Lightning Location Data Employing Measurements of Direct Strikes to a Radio Tower, CIGRE Session, Paris.

[5]   Herodotou, N., W. A. Chisholm, and W. Janischewskyj (1993), Distribution of lightning peak stroke currents in Ontario using an LLP system, IEEE transactions on Power delivery, Vol. 8, Nb. 3.

[6]   Idone, V. P., S. B. Arsalan, R. W. Henderson, P. K. Moore, and R. B. Pyle (1993), A Reexamination of the Peak Current Calibration of the National Lightning Detection Network, J. Geophys. Res. Vol. 98, No. D10, p. 18,323-18,332.

[7]   Jerauld, J., V. A. Rakov, M. A. Uman, K. J. Rambo, D. M. Jordan, K. L. Cummins, and J. A. Cramer (2005), An evaluation of the performance characteristics of the U.S. National Lightning Detection Network in Florida using rocket-triggered lightning, J. Geophys. Res., 110, D19106, doi:10.1029/2005JD005924.

[8]   Krider, E. P., R. C. Noggle, and M. A. Uman (1976), A gated wideband magnetic direction-finder for lightning return strokes, J. Appl. Meteor., (15), pp. 301–306.

[9]   Krider, E. P., R. C. Noggle, A. E. Pifer, and D. L. Vance (1980), Lightning direction finding systems for forest fire detection, Bull. Amer. Meteor. Soc., (61), pp. 980–986.

[10]   Orville, R. E. (1991), Calibration of a Magnetic Direction Finding Network Using Measured Triggered Lightning Return Stroke Peak Currents, J. Geophys. Res. Vol. 96, No. D9, p. 17,135-17,142.

[11]   Pichler, H., G. Diendorfer and M. Mair (2007), Correlated current and far field records from lightning discharges to the Gaisberg tower, IX International Symposium on Lightning Protection (SIPDA), Foz do Iguazo, Brazil

[12]   Rachidi, F., J. L. Bermudez, M. Rubinstein, and V. A. Rakov (2004), On the estimation of lightning peak currents from measured fields using lightning location systems, Journal of Electrostatics, Vol. 60, pp. 121-129.

[13]   Rakov, V. A., and M. A. Uman (2003), Lightning: Physics and Effects. Cambridge University Press.

[14]   Rakov V.A. (2007), Lightning Return Stroke Speed, Journal on Lightning Resarch (JOLR), Vol. 1 pp. 80-89

[15]   Schulz, W., and G. Diendorfer (2000), Evaluation of a lightning location algorithm using an elevation model, 25th International Conference on Lightning Protection (ICLP), Rhodos

[16]   Schulz, W., K. Cummins, G. Diendorfer, and M. Dorninger (2005), Cloud-to-ground lightning in Austria: A 10-year study using data from a lightning location system, J. Geophys. Res., 110, D09101, doi:10.1029/2004JD005332.

[17]   Uman, M. A., D. K. McLain, and E. P. Krider (1975), The electromagnetic radiation from a finite antenna, Am. J.Phys. 43.